

Energy extraction from ocean currents and waves: Mapping the most promising locations

Ana Ordonez

Academic Affiliation, Fall 2012: Undergraduate, Arizona State University

SOARS[®] Summer 2012

Science Research Mentor: Baylor Fox-Kemper, Peter Hamlington

Writing and Communication Mentor: Brian Bevirt

Community Mentor: McArthur Jones

Peer Mentor: Manny Hernandez

ABSTRACT

Concerns about fossil fuel supplies and an ever-increasing demand for energy have prompted the search for alternative power sources. One option is the ocean, a power-dense and renewable source of energy; but its capacity to meet human energy demands is poorly understood. While raw wave energy resources have been investigated at many scales, little is known about where and how much power can be extracted. Even less is known about the energy available in ocean currents, especially on a global scale. This study assessed where significant amounts of energy in ocean waves and currents are available for human use. Global wave and current energy were calculated from model data and mapped. To assess the recoverable energy around the United States, population and marine protected area data were combined with technical specifications for the Pelamis and SeaGen energy convertors, and the dollar values of the energy were estimated. The results suggest that promising amounts of wave and current energy are available both globally and around the United States. Potential locations for wave and current energy farms appear to exist on the Pacific, Atlantic, and Gulf Coasts of the U.S. Further research in this area may lead to greater support for developing, testing, and deploying ocean energy converter technology.

This work was performed under the auspices of the Significant Opportunities in Atmospheric Research and Science Program. SOARS is managed by the University Corporation for Atmospheric Research and is funded by the National Science Foundation, the National Oceanic and Atmospheric Administration, the Cooperative Institute for Research in Environmental Science, the University of Colorado at Boulder, and by the Center for Multiscale Modeling of Atmospheric Processes.

1. Introduction

Uncertainties and concerns about fossil fuel supplies and an ever-increasing demand for energy have prompted the search for alternative power sources. One option is ocean energy, a power-dense and renewable resource. A recent estimate shows that about 2.11 terawatts (TW) (Gunn and Stock-Williams 2012) of power exists in the waves alone. Waves, tides, currents, and gradients in temperature and salinity all have the ability to supply energy, and an abundance of prototype devices for converting ocean energy have been tested successfully (Bedard et al., 2008). While many devices are advancing from the prototype stage to commercial deployment, there is still a need for financial and political incentives to advance these young technologies (Esteban and Leary 2012). Ocean energy extraction could become competitive by the early 2020s and produce 7% of global electricity by 2050, but such success will depend on showing investors and governments that this energy can be harvested economically (Esteban and Leary 2012).

One way to mobilize this support is through comprehensive resource assessments. Many researchers, companies, and nations have studied the wave energy resources available on scales ranging from an individual bay to all of the oceans. One of the earliest global wave resource assessments is by R. Tornkvist, who calculated power from visual wave observations (Glendenning 1980). Barstow et al., (1998) used satellite altimeter measurements to estimate wave power along coasts, and Cornett (2008) and Gunn and Stock-Williams (2012) analyzed NOAA WAVEWATCH III model data to create spatially continuous global wave power maps.

Ocean current resource assessments are fewer in number. Open-ocean and tidal currents are a much denser source of power than wind, and tidal currents also have the advantage of being predictable. Bahaj and Myers (2003) note that tidal current installations could even provide a base load of electricity by using two separate arrays that have offset peak flows. Estimates have been made of the power available from tides and open-ocean currents in the United States (Duerr and Dhanak 2012, Georgia Tech 2011, U.S. Dept. of Interior 2006). There do not appear to be any studies published that assess the ocean current energy potential on a global scale.

It is necessary to understand how the spatial and temporal variations in energy-generating potential relate to existing technology, especially in terms of resource availability and funding. One of the biggest obstacles for developing this resource is cost per megawatt installed, which is higher for ocean energy than for other renewable sources (Bahaj 2011). While the oceans provide free energy potential, the high capital, operations, and maintenance costs of the power convertors can deter investors and delay development (Bahaj 2011). The intermittency of waves and currents is another challenge. There is also the issue that different types of convertors can respond to the same wave climate with different power outputs, so the results for one device may not provide the best picture of overall energy availability. Better knowledge of the global raw resource can suggest how much potential for ocean energy development exists in a region, but site-specific assessments are necessary before developing any one location (Gunn and Stock-Williams 2012, Bahaj 2011) For any device, it is very important to select sites with suitable physical characteristics that will also allow unattended devices to maximize energy production close to population centers. Understanding the geographic and temporal distributions of wave

and current energy and how they compare with other characteristics, such as water depth, is crucial for assessing the feasibility of energy extraction technologies.

The steps in this research first involve mapping the global distributions of wave and current energy resources. Model data is used to calculate wave energy transport, coastal wave energy flux, and current power using the equations and assumptions in the data and methods section. These raw data are then applied to an analysis of the power generated by wave and current farms around the U.S. The cost of installing and operating these energy farms is compared to the energy output and mapped as cost per megawatt. The results section features the maps of global wave and current energy resources along with wave and current farm output and cost per megawatt around the U.S. The maps are discussed and many directions for future work are identified.

2. Data and Methods

This section introduces the wave, ocean current, and auxiliary data sets and explains the procedures for calculating energy. It finishes with a description of the methods used to locate interesting areas and explore the temporal variations of energy in those locations.

a. Wave and Current Data

The wave data were generated from the NOAA WAVEWATCH III model (NOAA/NWS 2012) with the forcings described in section 3.5 of Webb and Fox-Kemper (2011). The grid cells have a $2.5^\circ \times 2.5^\circ$ resolution where latitude spans from -78° to 78° and longitude from 0° to 360° . A grid cell would be approximately 112 km x 112 km at the equator, and cell size decreases toward the poles. The data covers years 1994-2001 with a 6-hour time step. This study used the significant wave height (H_{m0}), the zero-crossing wave period (T_z), and the wave direction variables for calculations.

The ocean current model dataset is described in Grooms et al., (2011) and Fox-Kemper et al., (2012). The resolution varies in longitude, latitude, and depth. The variables used included the time mean flow kinetic energy, the eddy kinetic energy, and the mean zonal (U) and meridional (V) velocity components.

b. Wave Energy Calculations

The total energy transport (EC_g) was calculated by including both the kinetic and potential energy of the waves and using the deep water wave assumption for group velocity (Holthuijsen 2007):

$$\text{---} \tag{1}$$

Here ρ is the density of water (1000 kg m^{-3}), g is the acceleration due to gravity (9.81 m s^{-2}), T_z is the zero-crossing period, and H_{m0} is the spectral significant wave height. Ideally the energy period, T_e , would be used instead of T_z , but it was not available in this study's data. Dunnett and Wallace (2009) describe some commonly employed substitutions for T_e , such as

assuming that T_e is proportional to the mean zero-crossing period (T_z) or the peak period (T_p). The global wave energy estimates in Cornett (2008) used $T_e=0.9T_p$ with the acknowledgement that such assumptions will introduce uncertainty in the estimates. Here it is assumed that $T_e=T_z$, as T_z is available from the model data and this study is more interested in exploring the relative concentrations of energy than accurately estimating the magnitudes of wave power.

Energy transport is commonly expressed in terms of kilowatts per meter (kW m^{-1}). This is how wave energy is frequently quantified in wave resource assessments. Equation (1) is used in this study to calculate the energy transport for the grid introduced in section a.

c. Calculating Power Flow into Coasts

Near coastlines, the intricate interactions between waves, bathymetry, and shore topography complicate estimates of the energy transport. Methods exist to accomplish this task. In Pontes et al., (2005) a numerical wave model is connected to an inverse-ray model that considers effects such as shoaling and refraction. This detailed form of analysis is appropriate for investigating a site or even quantifying the wave resources of a country, but it is impractical to perform on a global scale with the amount of uncertainty in the energy transport analysis. The nature of wave power near coasts around the world is still interesting because wave energy convertors are generally designed for depths of 40-100 m (Scruggs and Jacob 2009), which usually occur near shores. To investigate this, the overall power flow into the coastlines was calculated at each grid cell bordering a coast.

The coast is defined as the border between ocean cells and cells with no data. Since the power density of each point, as calculated with equation (1), was assumed to travel in the mean wave direction at that grid point, it could be separated into components pointing in the cardinal directions. The component of the wave power density normal to each coastal cell border was calculated and multiplied over the total length of that boundary according to the equations below:

$$\text{---} \quad (2)$$

$$\text{---} \quad (3)$$

P_y is the power in the north or south direction, and P_x is for power in the east or west direction. Theta, θ , is the wave direction in degrees. When the coast was to the south or the west, θ was replaced with $\theta-180^\circ$ to keep the trigonometric functions consistent. If the waves in either direction were flowing away from the coast (a negative value), that component was considered to be zero.

The variables dx and dy are the zonal and meridional lengths of the cell, respectively. The height (dy) was assumed to be a constant 1.12×10^5 m per degree¹, while the length (dx) was calculated as:

¹ The decrease in cell heights at high latitudes does not create a significant error at this level of analysis

(4)

Phi (ϕ) is the latitude in degrees. Once P_x and P_y were calculated, they were added to get the total power flowing into the coast at that grid cell. An illustration of this method is shown in Figure 1.

d. Ocean Current Energy Calculations

The power (P) in a stream of water is given in Bahaj (2011) by:

$$P = \frac{1}{2} \rho A v^3 \quad (5)$$

where ρ is the density of water (1000 kg m^{-3}), A is the cross-sectional area of a rotor in the current (m^2), and v_0 is the speed of the stream (m s^{-1}).

The coarse volume-weighted mean flow energy and eddy energy values were summed to get the total kinetic energy. This value is in terms of v^2 rather than v^3 . To estimate v^3 , the total kinetic energy was raised to the $3/2$ power.

Each grid cell contains a certain volume of water, and equation (5) can calculate the energy flowing through a slice of that volume. To find the total power flowing through a grid cell, the following modification was made:

$$P_{\text{total}} = P \times V \quad (6)$$

V is the total volume of the cell. This was calculated by multiplying the area by the depth, both of which were provided in the dataset. The area of each cell varied, and the depth was 5.0062 m, which was the closest layer to the surface.

e. Wave Farm Output and Cost Estimation

Additional information about the ocean environment came from data on marine protected areas and bathymetry. Inventories of marine protected areas and *de facto* marine protected areas (locations where activities are restricted for reasons other than conservation) were downloaded as ESRI geodatabases from the National Marine Protected Areas (MPA) Data & Analysis webpage. Areas which would likely not allow installation of an energy farm were selected for mapping. The areas that were not classified as “Uniform Multiple Use” were extracted from the marine protected areas feature class. The areas that restricted all activity and those that restricted energy exploration and extraction were extracted from the *de facto* marine protected areas feature class. An ascii file of 10 minute bathymetry from the ETOPOP1 1-Minute Global Relief dataset was obtained using the GEODAS grid translator “Design a grid” tool (National Geophysical Data Center 2012). A grid was selected spanning from 18° to 75° N and -60° to -180° W.

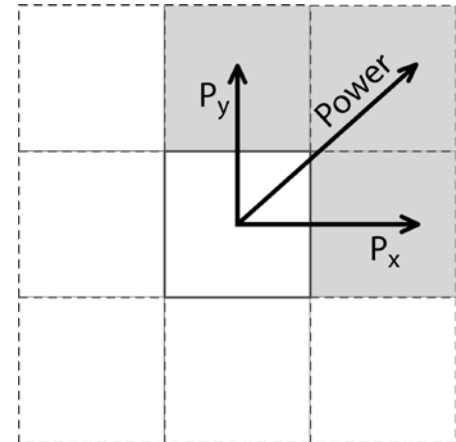


Fig. 1. An illustration of how coastal power is calculated. The shaded cells represent land area and the white cells are ocean. If the wave energy transport in the central cell is represented by the vector ‘Power’, then the wave power normal to the coast in this cell is equal to the sum of the components P_x and P_y .

Mean electricity consumption was calculated by multiplying population times the estimated mean consumption per person. The gridded population is from the Gridded Population of the World Version 3 dataset, available online from the Socioeconomic Data and Applications Center². It is adjusted to match U.N. totals. The dataset is documented at CIESIN (2012) and in Balk et al., (2010). The grid for the year 2000 was selected because it was the most recent density estimate that was not created from extrapolated population counts. The latitude ranged from -58° to 85°, which excludes Antarctica, and the longitude ranged from -180° to 180°. The mean electricity consumption at each population grid cell was estimated using 2009 energy data from the U.S. Energy Information Administration (EIA). The total energy consumption per household member was 34.8 million BTU, which is about a constant rate of 1.3 kW over the whole year. Multiplying this by the number of people in each cell produced the mean consumption data.

It was assumed that the energy convertors would be installed in farms. The Pelamis³ wave energy convertor was chosen as the device installed in the wave energy farm. The SeaGen S⁴ turbine was chosen for the marine current turbine. These devices were selected because sufficient information could be found to estimate the output and cost of the respective farms.

The wave farm consisted of 30 devices rated at 750 kW for a total capacity of 22.5 MW. The current farm consisted of 15 devices rated at 1.2 MW for a total capacity of 18 MW. The energy outputs from the Pelamis and SeaGen devices were estimated using data from the manufacturers along with data on the depth and speed of the water. A Pelamis power matrix (Dalton et al., 2009) provided the output in kW for each combination of spectral wave height and zero-crossing period, and the results were multiplied by 30 for each grid cell. Table 1 in Douglas et al., (2007) provided information on the rated output, rated speed, cut-in speed, and capacity factor of the SeaGen turbine. Substituting these into equation (6) along with the v_0 ³ estimated in section 2d. provided an estimate of the mean power, in watts, that could be generated by the SeaGen device. This was multiplied by 15 for each cell to get the power generated by the farm. It was assumed that both types of farm would operate for 20 years (Douglas 2008, Dunnett and Wallace 2009).

Once the output of the farms was calculated, the range of suitable locations was mapped by finding areas that satisfied the devices' operating requirements. ArcMap was used to perform this part of the analysis. The wave farm needed to be in depths greater than 50 m to operate. The bathymetry grid was reclassified according to the wave farm values in Table 1, then the raster calculator tool was used to multiply the reclassified bathymetry by the wave farm energy, with the resulting raster generated at the resolution of the bathymetry. It was re-aggregated to the wave energy's original 2.5 x 2.5° resolution using the Aggregate tool, which assigned the mean of the energy values to each new cell.

² <http://sedac.ciesin.columbia.edu/gpw>

³ <http://www.pelamiswave.com>

⁴ <http://www.marineturbines.com>

The marine current farm range was determined by depth and current speed. The current energy was interpolated to a $1^\circ \times 1^\circ$ grid using Matlab's `triscatteredinterp` function with nearest neighbor interpolation and saved to an ascii file that was opened in ArcMap. While the SeaGen device is designed for depths of 25 – 2 m (Wright 2008), the range was increased in this analysis because the current energy grid was very coarse compared to the bathymetry grid. The mean current speed was calculated from the mean U and V velocity components in the current model dataset. These values were also interpolated onto a $1^\circ \times 1^\circ$ grid. The bathymetry and current speeds were reclassified according to the values in Table 1. The raster calculator tool was used to multiply the reclassified bathymetry and speed by the energy to obtain the spatial extent of “recoverable” energy. Two different cut-in speeds (the lowest speed at which the turbine will generate electricity) were tested. The first is the SeaGen cut-in speed of 0.7 m s^{-1} , and the second is a very low cut-in speed of 0.3 m s^{-1} , such as that for the low cut-in speed of the vertical-axis Darrieus turbine tested in Alam and Iqbal (2010).

	Required Depth	Cut-In Speed	Rated Speed
Wave farm	> 50 m	N/A	N/A
Current farm	20 – 1000 m	0.7 m s^{-1} , 0.3 m s^{-1}	2.25 m s^{-1}

Table 1. These are the depths and current speeds used to determine where the farms could operate.

The cost estimate of the farms considered the transmission line, capital, and operations and maintenance (O&M) costs. The subsea transmission system was assumed to be an HVDC VSC (high voltage direct current voltage source convertor), and the costs were calculated based on the equations in section 5.3 of de Alegría et al., (2008), assuming a cable rated for 440 kV. While HVAC is currently a cheaper option for connections less than 50 km from shore, HVDC has many technical advantages and no distance limit (de Alegría et al., 2008). The value was converted from pounds to U.S. dollars (Internal Revenue Service 2012) and rounded to \$280,000 km^{-1} , including the installation cost. Since the cost depends on distance from the coast, a shapefile of the boundaries of North America was obtained from the North American Atlas through the Geo.Data.gov portal. To get the cost of installing a cable to each point, the Euclidian distance tool in ArcMap 10 was run to find the distance in kilometers from any cell to the shapefile of North America. This distance was multiplied by the cable cost per kilometer.

The capital and O&M cost for the wave farm were estimated using rates from Table 17 of Dunnett and Wallace (2009). The capital and operations costs were given in costs per kilowatt, which were multiplied by the total kilowatt capacity of the hypothetical wave farm. The SeaGen farm's capital cost was estimated using table 8.3 of DTI (2007), and O&M costs came from table 8.4. For the capital cost here, the grid connection estimate was subtracted from the total farm cost estimate since it would be accounted for by the cable expense. The resulting cost per megawatt capacity was multiplied by the farm capacity and converted to U.S. dollars to obtain the final capital expense. For both the wave and current farms, the total cost of the farm at each location was obtained by adding the total cable cost to the capital and O&M costs. The total costs were then divided by the estimated mean output in megawatts to obtain a total cost per megawatt.

	Wave farm	Current farm
Capital	\$93,487,500	\$21,560,000
O&M	\$37,080,180	\$25,670,000
Total	\$130,567,680	\$47,230,000

Table 2. The capital and operations and maintenance values used to calculate the cost per megawatt of each farm type.

3. Results

a. Waves

The global wave energy transport and coastal wave energy flux (Figs. 2 and 3) followed general patterns of having higher values in the mid-latitudes and on the west coasts of continents. The lowest values are in equatorial waters near landmasses and in Polar regions that experience seasonal ice cover.

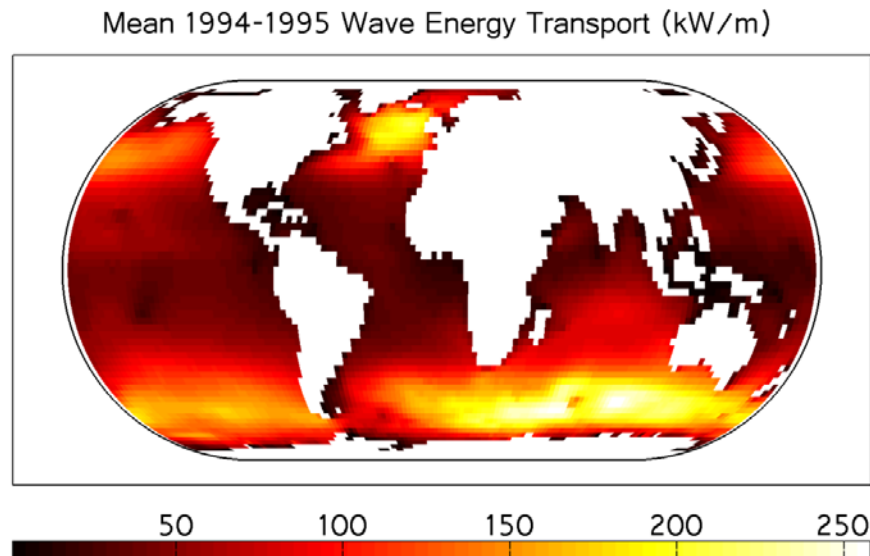


Fig. 2. Global wave energy transport as calculated in section 2b, shown in kW m^{-1} using an Eckert IV equal-area projection. The highest wave energy transport values are in the mid-latitudes, particularly in the north Atlantic and in the south Indian Oceans.

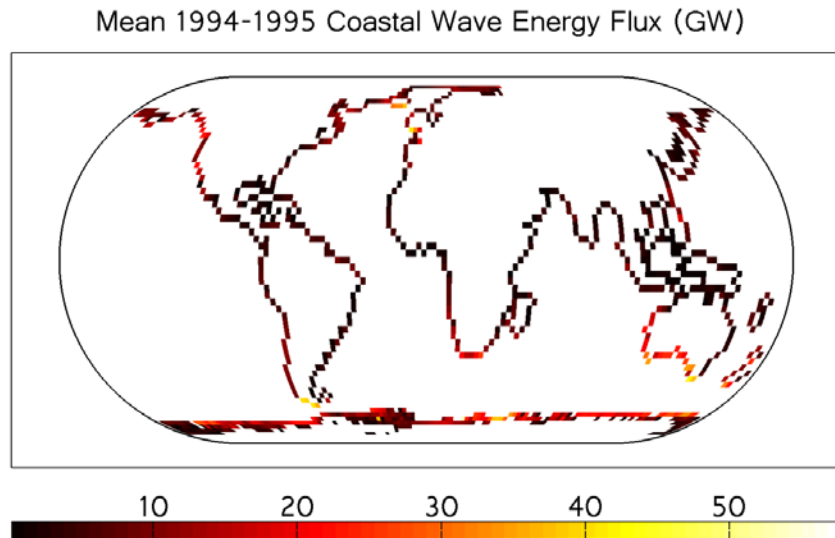


Fig. 3. The global coastal wave energy flux calculated in section 2c, shown in gigawatts (GW) on an Eckert IV equal-area projection. The regions with greatest energy are the west coasts of North America and Europe, the southwest coasts of South America and Africa, the south and west coast of Australia and New Zealand, and around Iceland and the eastern Philippines.

The spectral significant wave height and zero-crossing period from the global wave data were used to calculate the expected output of a wave farm with 30 Pelamis wave energy convertors, based on a Pelamis power matrix. Fig. 4 shows this result for the United States in relation to electricity consumption rates on land.

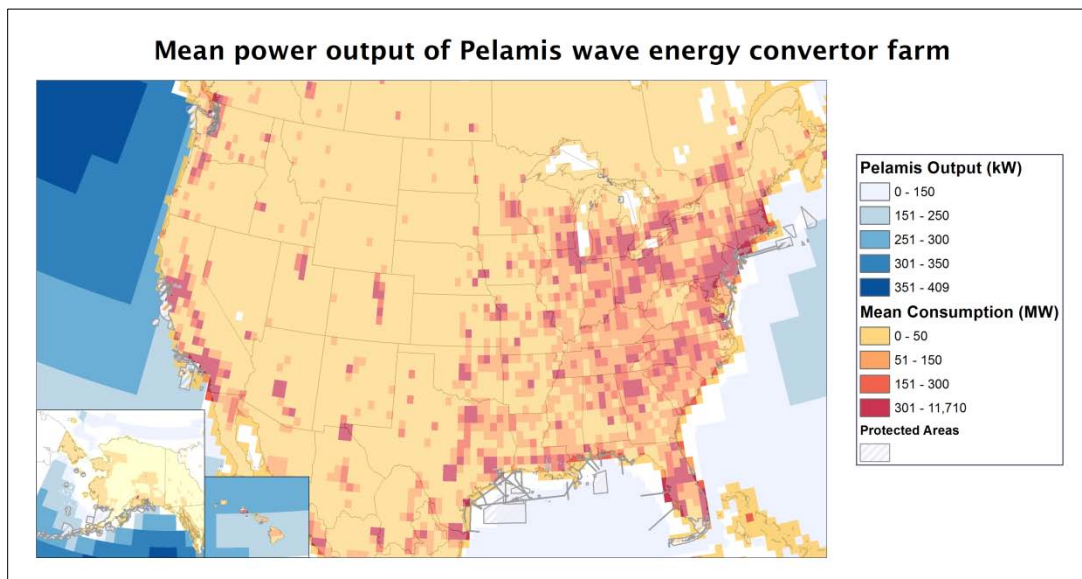


Fig. 4. Based on wave energy available, blue areas show the theoretical output of a wave farm with 30 Pelamis wave energy convertors. Electricity consumption rates are mapped on the land areas. Higher power could be harvested closer to the shore on the West Coast of the U.S. and off Alaska and Hawaii, but the estimated energy consumption onshore is less dense in these areas than on the East Coast.

The highest wave farm output values are in the range of 351–409 kW, found in the north Pacific. The West Coast has mean values of 151–350 kW. The Atlantic and Gulf Coasts fall in the 0–150 kW range, with the output increasing farther out to sea. The accessible energy is also farther offshore for the East Coast. However, the estimated energy consumption is greater on the East Coast and lower on the West Coast.

b. Currents

The energy in currents is not as widely distributed as that in waves, instead being concentrated in discrete streams around the world (Fig. 5). Some highly visible currents include the Gulf Stream, Agulhas Current, Kuroshio Current, and equatorial currents and countercurrents. While the energy in these currents can reach almost 20 MW or higher, the energy in most of the oceans is around 1 MW or less. Still, many of these energetic currents are near coasts, which makes them more accessible for harvesting and transmitting the power that could be generated there.

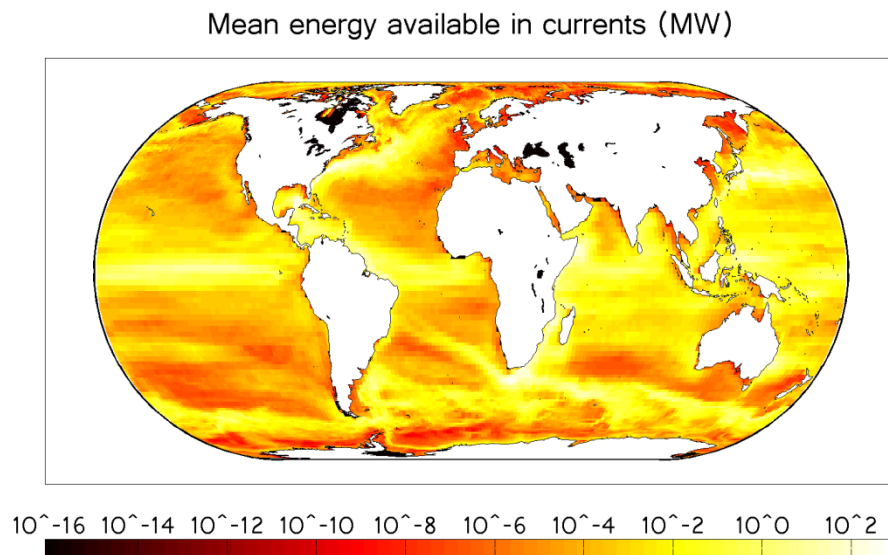


Fig. 5. The surface energy in currents as calculated in section 2d, shown in megawatts (MW) on an Eckert IV equal-area projection. Several large, distinct currents are visible, while the rest of the ocean has less energy in slower waters.

With the most relaxed restrictions of a cut-in speed of 0.3 m s^{-1} and a depth range of 20 – 1000m, the area of recoverable energy is still limited to the Southeast U.S. Coast. The highest output is in the Florida Strait, where a maximum value of 116,876 kW can be found. Nowhere around the U.S. were the currents as fast as the turbine's rated speed of 2.25 m s^{-1} . The fastest current speed in the Florida Strait was about 1.17 m s^{-1} .

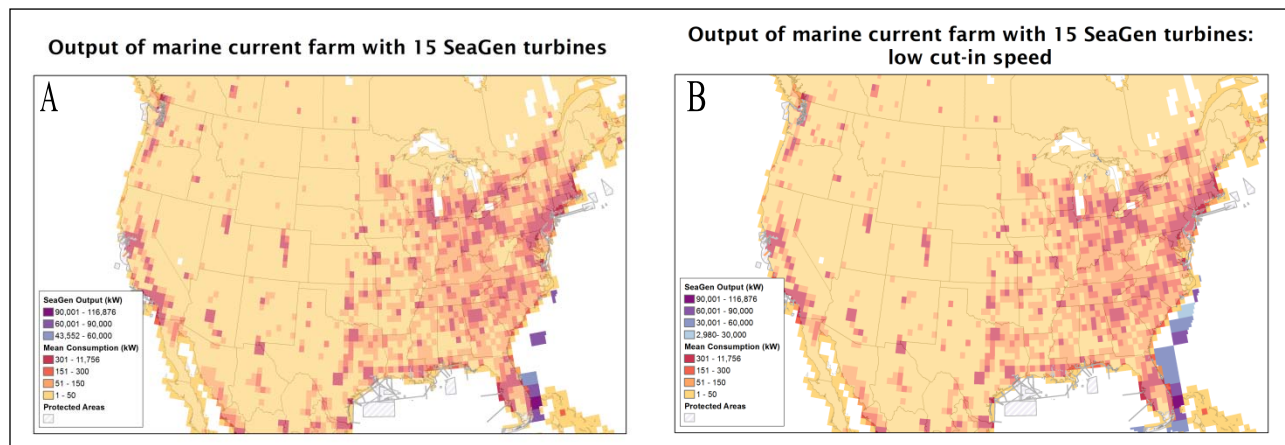


Fig. 6. Comparison of the current farm output and range with (A) the SeaGen's cut-in speed of 0.7 m/s and (B) a much lower cut-in speed of 0.3 m/s (presumed possible with technical advancements). Even with a low cut-in speed, the farm is limited to areas off the southeast coast of the U.S.

c. Comparing Output With Cost

Fig.7 accounts for the estimated cost of installing and running farms of each device. Both the East and West Coasts of the United States have areas in which a wave farm could be installed at relatively low cost, but these areas are much closer to the shore on the Pacific coast. The Gulf of Mexico sees higher costs per megawatt and also more protected areas. Marine current turbines could be installed off the southeast Atlantic Coast and in the Strait of Florida. Fig. 6 shows that elsewhere around the country, the water is either too deep or the currents too far below a cut-in speed of 0.3 m s^{-1} , which is already below the SeaGen's cut-in speed of 0.7 m s^{-1} .

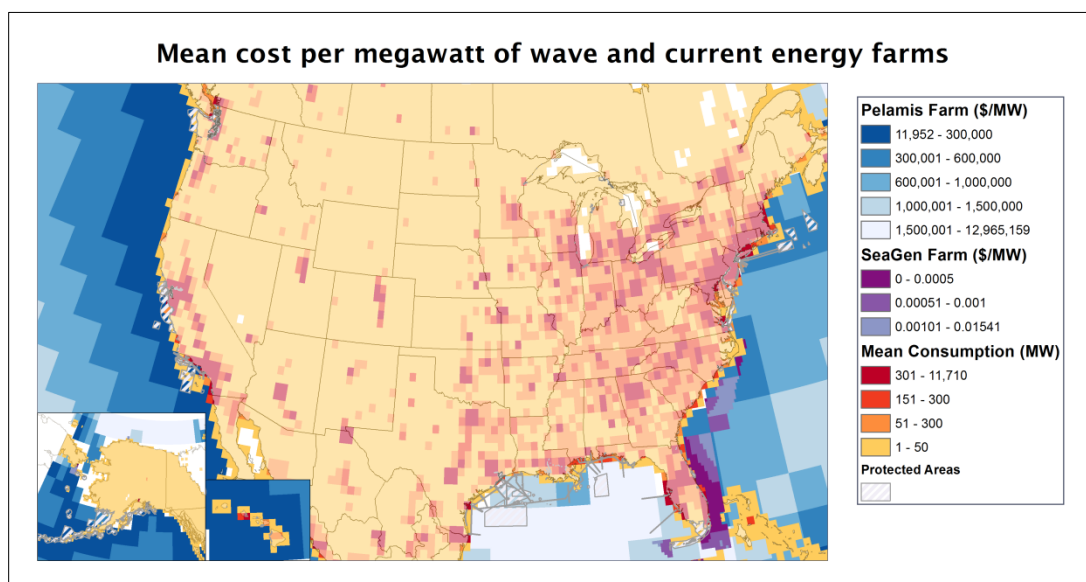


Fig. 7. Lifetime cost per megawatt capacity of the wave and current farms. Near-shore locations with high energy outputs, such as the West Coast, tend to be the least expensive. However, some less-energetic areas, such as the Mississippi Delta and east of North Carolina, are also in the lower-cost ranges.

4. Discussion

The wave energy averaged for 1994–1995 generally resembles the mean global distribution in Cornett (2008) though the values in Fig. 2 appear to be larger. For example, the middle Indian Ocean has values around 100 kW m^{-1} in Fig. 2, but only $50\text{--}60 \text{ kW m}^{-1}$ in Cornett (2008). This study only averaged two years of data, 1994–1995, while Cornett (2008) used 10 years, from 1997–2006. Averaging a longer period could explain the difference in mean energy transport range.

The qualitative analysis of the energy flux in Fig. 3 shows that the west coasts of North America and Europe, the southwest coasts of South America, Africa, and Australia, and parts of Iceland and the Philippines have especially high wave energy resources. Gunn and Stock-Williams (2012) also calculated the coastal wave energy flux for the world's coasts and used it to determine the wave resource for specific continents and countries. Their method involved calculating the energy crossing a line buffered from the coast, while this study added the components of the mean wave energy flowing into each side of a coastal grid cell. The total energy flux for each country was not calculated, but such an estimate could be obtained from these data and compared with those in other studies. This estimation would not include energy in waves generated by tropical storms, tsunamis, landslides, and other sources which are not resolved by the NOAA WAVEWATCH III model (NOAA/NWS).

A comparison of the wave farm output (Fig. 4) and cost per megawatt (Fig. 7) show that the energetic areas off the west coast are relatively inexpensive, and also reveal that harvesting less energetic areas may be cost-effective. Off both the East and Gulf Coasts, the output is in the $0\text{--}150 \text{ kW}$ range. While the cost of installing and running a wave farm on the Gulf Coast ranges from $\$600,001\text{--}12,965,159$ per MW, the cost on the East Coast only ranges from $\$300,001\text{--}1,000,000$ per MW. While the costs are rough estimates that only address a few budget items, this analysis demonstrates both the complexity of assessing the value of extractable energy at a site and how this framework of oceanographic data processing and GIS tools can be used to address it.

In analyzing the output of a marine current energy farm, generous limits were allowed for the depth and speed requirements. A depth range greater than that required by the SeaGen turbine was allowed both because of the coarseness of the current data when compared to the bathymetry and the expectation that future turbines will be deployable in deeper waters. The results in Figs. 4 and 6 suggest that current farms could generate more power than wave farms around the U.S. The greatest current farm output in Fig. 6 is almost 3,000 times larger than the highest wave farm output in Fig. 4. There will be some error in the current farm output because of the method used to estimate the velocity cubed term in the equation (described in section 2d), though the amount of error was not investigated. More investigation is needed to compare the amount of power generated by current farms to that of wave farms. The cost per megawatt analysis used the marine current farm output results with the lower cut-in speed. Despite these more relaxed limits, suitable areas for the marine current farm were still limited to the Florida Strait and nearby areas off the East Coast (Fig. 6). This area has long been recognized as a promising location for extracting energy from the Gulf Stream (Hanson et al., 2010), but energy is also contained in slower currents all around the U.S. Based on these results, it appears that

future turbines will need to be able to operate in deeper waters or at lower speeds to have more practical applications in the U.S.

Considering the global current energy distribution in Fig. 5, this may apply to current energy extraction at many other locations around the world where the energy in currents is at 5 MW or less. According to the Massachusetts Executive Office of Energy and Environmental Affairs, an offshore 1 MW wind turbine could power about 500 homes. While the power output of a marine current turbine will depend greatly on the speed and consistency of the currents, even the less-energetic areas have the potential to contribute useful power when the developing technology becomes capable of extracting it.

The cost estimates are very coarse and are most valuable as an approach for future analyses. The cable, operations, and maintenance costs are mostly based on models rather than actual energy farm operations experience. The cost of the SeaGen farm was based on estimates for a slightly different set-up of thirty 1 MW devices (DTI 2007). The O&M costs for the Pelamis convertor were estimated in Dunnett and Wallace (2009) by assuming that the device operates at a mean capacity of 20%, and that the O&M would be 2% of the capital expenditures. A complete cost assessment would need to include many other items, such as decommissioning and even the layout of the farm, as done for example in Allan et al., (2011), Beels et al., (2011), and DTI (2007). Higher-resolution wave and current data would also be more appropriate for a thorough assessment of the energy resources for a nation or region. Fig. 7 provides an example of how these forms of data may be combined to assess recoverable energy. The GIS methods used to perform this analysis allow for better data to be substituted into the framework already being developed.

5. Conclusions

Spectral wave data from the NOAA WAVEWATCH III model were used to calculate energy transport in the world's oceans and the energy flux into the world's coastlines, and the patterns were similar to those seen in other wave energy studies. Data from another model were used to estimate the energy in the world's currents. Most of the energy was found to be concentrated in several large currents, and small amounts of energy were distributed throughout the rest of the oceans. The resources around the United States were analyzed in greater detail. Locations of recoverable energy were found by estimating the outputs of the Pelamis wave energy convertor and the SeaGen S marine current turbine. The cost of installing and maintaining a farm of devices at each grid cell was estimated and compared to the potential power generation.

Farms of Pelamis devices could be productive on both the Atlantic and Pacific Coasts of the U.S. While the Pacific Ocean is more energetic, the cost per megawatt of energy produced is still comparable to that of many near-shore areas in the Atlantic. The SeaGen turbine was only effective off the southeast coast of the United States, especially in the Strait of Florida. It was limited by both the shallow depths and having a cut-in speed higher than the majority of current speeds.

There are many ways to improve on this study. The wave energy was only averaged for two years, and while the spatial patterns of the results compared well with another study, the values were skewed higher. More years of data should be included. The current model could be re-run to output a mean velocity cubed, which will increase the accuracy of the energy quantities shown. Higher-resolution models could be run to study the energy output in smaller regions. More geographic data can be included, and a much more rigorous process can be developed to estimate the cost and eventually assign an economic value to the resources at each location. Finally, the environmental impacts of these technologies will require further study, especially before they are deployed near ecologically sensitive areas. The results of this study provide an overview and starting point for more refined, in-depth research.

References

- Alam, J. and T. Iqbal, 2010: A low cut-in speed marine current turbine. *Journal of Ocean Technology*, **5**, 49-62.
- Allan, G., M. Gilmartin, P. McGregor, and K. Swales, 2011: Levelised costs of Wave and Tidal energy in the UK: Cost competitiveness and the importance of ‘banded’ renewables obligation certificates. *Energy Policy*, **39**, 23–39, doi:10.1016/j.enpol.2010.08.029.
- Bahaj, A. S., 2011: Generating electricity from the oceans. *Renewable and Sustainable Energy Reviews*, **15**, 3399–3416, doi:10.1016/j.rser.2011.04.032.
- , and L. Myers, 2003: Fundamentals applicable to the utilisation of marine current turbines for energy production. *Renewable Energy*, **28**, 2205–2211, doi:10.1016/S0960-1481(03)00103-4.
- Balk, D., G. Yetman, and A. D. Sherbinin, 2010: Construction of Gridded Population and Poverty Data Sets from Different Data Sources. Proceedings, *European Forum for Geostatistics Conf.*, Tallinn, Estonia, European Forum for Geostatistics, 12–20.
- Barstow, Stephen F., Ola Haug, and Harald E. Krogstad, 1998: Satellite altimeter data in wave energy studies. *Proceedings of the Third International Symposium Waves 97*, Virginia Beach, Va., American Society of Civil Engineers, 339-354.
- Bedard, R., P. T. Jacobson, M. Previsic, W. Musial, and R. Varley, 2008: An Overview of Ocean Renewable Energy Technologies. *Oceanography*, **23**, 22–31.
- Beels, C., P. Troch, J.P. Kofoed, P. Frigaard, J.V. Kringelum, P.C. Kromann, M.H. Donovan, J. De Rouck, and G. De Backer, 2011: A methodology for production and cost assessment of a farm of wave energy converters. *Renewable Energy*, **36**, 3402–3416, doi:10.1016/j.renene.2011.05.019.
- CIESIN (Center for International Earth Science Information Network), Columbia University; and Centro Internacional de Agricultura Tropical (CIAT), cited 2012: Gridded Population of the World, Version 3 (GPWv3): Population Density Grid. [Available online at <http://sedac.ciesin.columbia.edu/gpw> .]
- Cornett, A.M., 2008: A Global Wave Energy Resource Assessment. Proceedings, *18th International Offshore And Polar Engineering Conf.*, J.S. Chung, Ed., Vancouver, Canada, International Society of Offshore and Polar Engineers, 1–9.
- Dalton, G.J., R. Alcorn, and T. Lewis, 2010: Case study feasibility analysis of the Pelamis wave energy convertor in Ireland, Portugal and North America. *Renewable Energy*, **35**, 443–455, doi:10.1016/j.renene.2009.07.003.

- de Alegría, I.M., J.L. Martín, I. Kortabarria, J. Andreu, and P.I. Ereño, 2009: Transmission alternatives for offshore electrical power. *Renewable and Sustainable Energy Reviews*, **13**, 1027–1038, doi: 10.1016/j.rser.2008.03.009.
- DTI, 2007: Economic viability of a simple tidal stream energy capture device. DTI Project No: TP/3/ERG/6/1/15527/REP, 73 pp.
- Duerr, A.E.S., and M.R. Dhanak, 2012: An Assessment of the Hydrokinetic Energy Resource of the Florida Current. *IEEE J. Oceanic Engineering*, **37**, 281–293, doi:10.1109/JOE.2012.2186347.
- Dunnett, D. and J. Wallace, 2009: Electricity generation from wave power in Canada. *Renewable Energy*, **34**, 179–195, doi: 10.1016/j.renene.2008.04.034.
- EIA (U.S. Energy Information Administration), cited 2012: 2009 RECS Survey Data, Totals and Intensities, U.S. Homes, (CE1.1). [Available online at <http://www.eia.gov/consumption/residential/data/2009/#consumption-expenditures> .]
- Esteban, M., and D. Leary, 2012: Current developments and future prospects of offshore wind and ocean energy. *Applied Energy*, **90**, 128–136, doi:10.1016/j.apenergy.2011.06.011.
- Fox-Kemper, B., R. Lumpkin, and F. O. Bryan, 2012: Lateral transport in the ocean interior. *Ocean Circulation and Climate - Observing and Modelling the Global Ocean*, G. Siedler, J. Church, J. Gould, and S. Griffies, Eds., Elsevier, Amsterdam. Submitted.
- Georgia Tech Research Corp., 2011: Assessment of Energy Production Potential from Tidal Streams in the United States. Final Proj. Rep. DE-FG36-08GO18174, 109 pp.
- Glendenning, I., 1980: Wave energy. *IEE Proceedings*, **127**, 301–307. doi: 10.1049/ip-a-1:19800048.
- Grooms, I., K. Julien, and B. Fox-Kemper, 2011: On the Interactions Between Planetary Geostrophy and Mesoscale Eddies. *Dynam. Atmos. Oceans*, **51**, 109–136, doi:10.1016/j.dynatmoce.2011.02.002.
- Gunn, K., and C. Stock-Williams, 2012: Quantifying the global wave power resource. *Renewable Energy*, **44**, 296–304, doi:10.1016/j.renene.2012.01.101.
- Hanson, H. P., S. H. Skemp, G. M. Alsenas, and C. E. Coley, 2010: Power from the Florida Current: A New Perspective on an Old Vision. *Bull. Amer. Meteor. Soc.*, **91**, 861–866, doi:10.1175/2010BAMS3021.1.
- Holthuijsen, L.H., 2007: *Waves in Oceanic and Coastal Waters*. Cambridge University Press, Cambridge, U.K., 417 pp.

- Internal Revenue Service, U.S. Dept. of the Treasury, cited 2012: Yearly Average Currency Exchange Rates. [Available online at <http://www.irs.gov/businesses/small/international/article/0,,id=206089,00.html> .]
- Massachusetts Executive Office of Energy and Environmental Affairs, cited 2012: Wind Energy: Facts. [Available online at <http://www.mass.gov/eea/energy-utilities-clean-tech/renewable-energy/wind/wind-energy-facts.html> .]
- National Marine Protected Areas Center (MPA), cited 2012: DeFacto Marine Protected Areas ESRI geodatabase. [Available online at <http://www.mpa.gov/dataanalysis/defacto/> .]
- , cited 2012: The Marine Protected Areas Inventory ESRI geodatabase. [Available online at <http://www.mpa.gov/dataanalysis/mpainventory/> .]
- National Geophysical Data Center (NGDC), cited 2012: GEODAS Grid Translator - Design-a-Grid. [Available online at http://www.ngdc.noaa.gov/mgg/gdas/gd_designagrid.html# .]
- NOAA/NWS Environmental Modeling Center, cited 2012: WAVEWATCH III Model. [Available online at <http://polar.ncep.noaa.gov/waves/wavewatch/wavewatch.shtml> .]
- North American Atlas, Instituto Nacional de Estadística Geografía e Informática, Natural Resources Canada, U.S. Geological Survey, cited (2012): North American Atlas - Political Boundaries. [Available online at http://dds.cr.usgs.gov/pub/data/nationalatlas/bound0m_shp.tar.gz .]
- Pontes, M.T., R. Aguiar, and H.O.Pires, 2005: A Nearshore Wave Energy Atlas for Portugal. *Journal of Offshore Mechanics and Arctic Engineering*, **127**, 249, doi:10.1115/1.1951779.
- Scruggs, J., and P. Jacob, 2009: Harvesting ocean wave energy. *Science*, **323**, 1176–1178, doi:10.1126/science.1168245.
- U.S. Dept. of Interior, 2006: Technology White Paper on Ocean Current Energy Potential on the U.S. Outer Continental Shelf. 7 pp.
- Webb, A., and B. Fox-Kemper, 2011: Wave spectral moments and Stokes drift estimation. *Ocean Modelling*, **40**, 273–288, doi:10.1016/j.ocemod.2011.08.007.
- Wright, M., 2008: The Development of the SeaGen Tidal Stream Turbine: Installation. [Available online at http://www.all-energy.co.uk/userfiles/file/Martin_Wright220508.pdf .]